Arabian Journal of Chemistry (2023) **16**, 104441

King Saud University

Arabian Journal of Chemistry

www.ksu.edu.sa
www.sciencedirect.com

ORIGINAL ARTICLE

Qingqianliusus A-N, 3,4-*seco*-dammarane triterpenoids from the leaves of *Cyclocarya paliurus* and their biological activities

Zhuliang Chen, Qian Wu, Jia Wu, Yong Yang, Yupei Yang, Qingling Xie, Leping Liu, Bin Wang, Yixing Qiu, Huanghe Yu, Wenbing Sheng, Yuqing Jian *, Wei Wang *

TCM and Ethnomedicine Innovation & Development International Laboratory, Innovative Materia Medica Research Institute, School of Pharmacy, Hunan University of Chinese Medicine, Changsha, Hunan 410208, People's Republic of China

Received 2 June 2022; accepted 13 November 2022
Available online 21 November 2022

KEYWORDS

Cyclocarya paliurus;
Juglandaceae;
Qinqianliusu;
3 4-*seco*-dammarane triterpenoids;
Anti-hypoglycemic;
Anti-inflammatory

Abstract Fourteen previously unreported 3,4-*seco*-dammarane triterpenoids named Qingqianliusus A-N (**1**–**14**), along with four known 3,4-*seco*-dammarane triterpenoid derivatives (**15**–**18**) were isolated from the 95 % ethanol extract of the *Cyclocarya paliurus* leaves. Compounds **1** and **2** possess a rare 3,11-heptacyclic lactone as natural product, and several pairs of the 3,4-*seco*-dammarane triterpenoid epimers with *R*/*S* configuration at C-24 were investigated and determined in detail for the first time. Compounds **8**, **11**, and **14** showed good α-glucosidase inhibitory effects with IC_{50} values of 4.97 ± 0.63, 7.08 ± 0.53, and 3.76 ± 0.77 μM, respectively. Meanwhile, compound **11** was also found potent inhibition rate of 35.83 % against COX-2, as compared with the positive control celecoxib (70.28 %). In addition, compounds **3**, **7**, **10**, and **13** exhibited outstanding cytotoxicities against human gastric cancer cell lines (BGC-823) with IC_{50} values of 7.69 ± 0.21, 8.47 ± 0.41, 9.04 ± 0.61, and 8.86 ± 0.38 μM, respectively. Compounds 1**3** and **3** had modest activities on human colon cancer cell lines (HCT-116) with IC_{50} values of 8.80 ± 0.36 and 9.45 ± 0.93 μM, respectively.

1. Introduction

Cyclocarya paliurus (Batalin) Iljinskaja (family: Juglandaceae), also known as "Qingqianliu" in Chinese, is now widely distributed in most areas of the south of the Yangtze River such as Hunan, Jiangxi, Hubei, Jiangxi, Sichuan, Guizhou, Guangxi, and Yunnan (Xie et al., 2010; Yang et al., 1992). As a precious species, its leaves have long history of being used as food resources and health care medicines. In Hunan folk medicine, Qingqianliu were used to slake thirst as a drink, and also called *Sweet Tea* due to sweet taste (Kennelly et al., 1995). More-

* Corresponding author.
E-mail addresses: cpujyq2010@163.com (Y. Jian), wangwei402@-hotmail.com (W. Wang).

Peer review under responsibility of King Saud University.

Production and hosting by Elsevier

https://doi.org/10.1016/j.arabjc.2022.104441
1878-5352

over, according to the "Resources of Traditional Chinese Medicine", it has the potential therapy to clear heat, reduce swelling and relieve pain. In August 2013, Qingqianliu also were approved by the National Health Commission of the People's Republic of China to become a new raw food material (Xie et al., 2015; Xie et al., 2018). Until 2017, Many enterprises exploited and developed the leaves of the title plant into health products with health care function of blood sugar, blood lipids, and blood pressure regulations, together with weight loss (https://db.yaozh.com/baojian).

In our previous study, >210 compounds have been reported from the title plant (Chen et al., 2022). Among them, the largest number of characteristic 3,4-*seco*-dammarane triterpenoids could be proved as quality markers to identify the plant (Cui and Li, 2012). They can also be considered as the major active and functional constituents in Qingqianliu with anti-hyperglycemic (Li et al., 2021; Li et al., 2012; Sun et al., 2020b; Yang et al., 2018; Zhou et al., 2021), anti-inflammatory (Li et al., 2021; Liu et al., 2020), cytotoxic (Chen et al., 2018; Sun et al., 2020a; Zhou et al., 2021), anti-hyperlipidemic (Wu et al., 2017; Yang et al., 2018), and anti-microbial (Kennelly et al., 1995) activities. Obviously, our previous researches have illustrated the cytotoxic capability of 3,4-*seco*-dammarane triterpenoids isolated from 80 % ethanol extract of Qingqianliu (Chen et al., 2018). The aim of this study focused on further chemical constituents and pharmacological activities to provide deeper insights into Qingqianliu as a nutraceutical additive or raw food material (Ning et al., 2019; Xie et al., 2018). On this basis, fourteen undescribed 3,4-*seco*-dammarane triterpenoids (**1**–**14,** Fig. 1) were extracted and separated from the chloroform extract of Qingqianliu. Moreover, their structures were elucidated through X-ray crystallography and extensive spectroscopic methods. Compounds (**1**–**14**) were tested for their biological properties on α-glucosidase inhibition, COX-2 inhibition, and cytotoxic activities.

2. Material and methods

2.1. General and solvents

UV spectra were recorded with Hewlett-Packard 8452A, UV–vis spectrophotometer (L.P., Palo Alto, Ca, USA). Using a Frontier infrared spectrometer to record IR spectra (PerkinElmer, U.S.A). HR-ESI-MS spectra were performed on Xevo G2-S QTOF mass spectrometer (Waters Co., Milford, MA, USA), 6500 series Q-TOF mass spectrometer (Agilent Co., USA) and LTQ Orbitrap Velos Pro MS (Thermo Scientific, MA, USA). The single Crystal X-ray diffraction data were obtained using a SuperNova, Dual, Cu at zero, AtlasS2 diffractometer (Rigaku Co., Japan). 1D and 2D NMR spectra were acquired on a Bruker Avance DRX-600 MHz spectrometer (Bruker Co., Billerica, MA, USA) at room temperature with CD_3OD as solvent. The absolute configuration of the sugar moiety was detected by HPLC analysis at 210 nm using C18 columns (5 μm, 4.6 × 250 mm, Agilent, Palo Alto, CA, USA) on Agilent 1260 series HPLC instrument (Agilent, Palo Alto, CA, USA). Semi preparative HPLC was carried out on

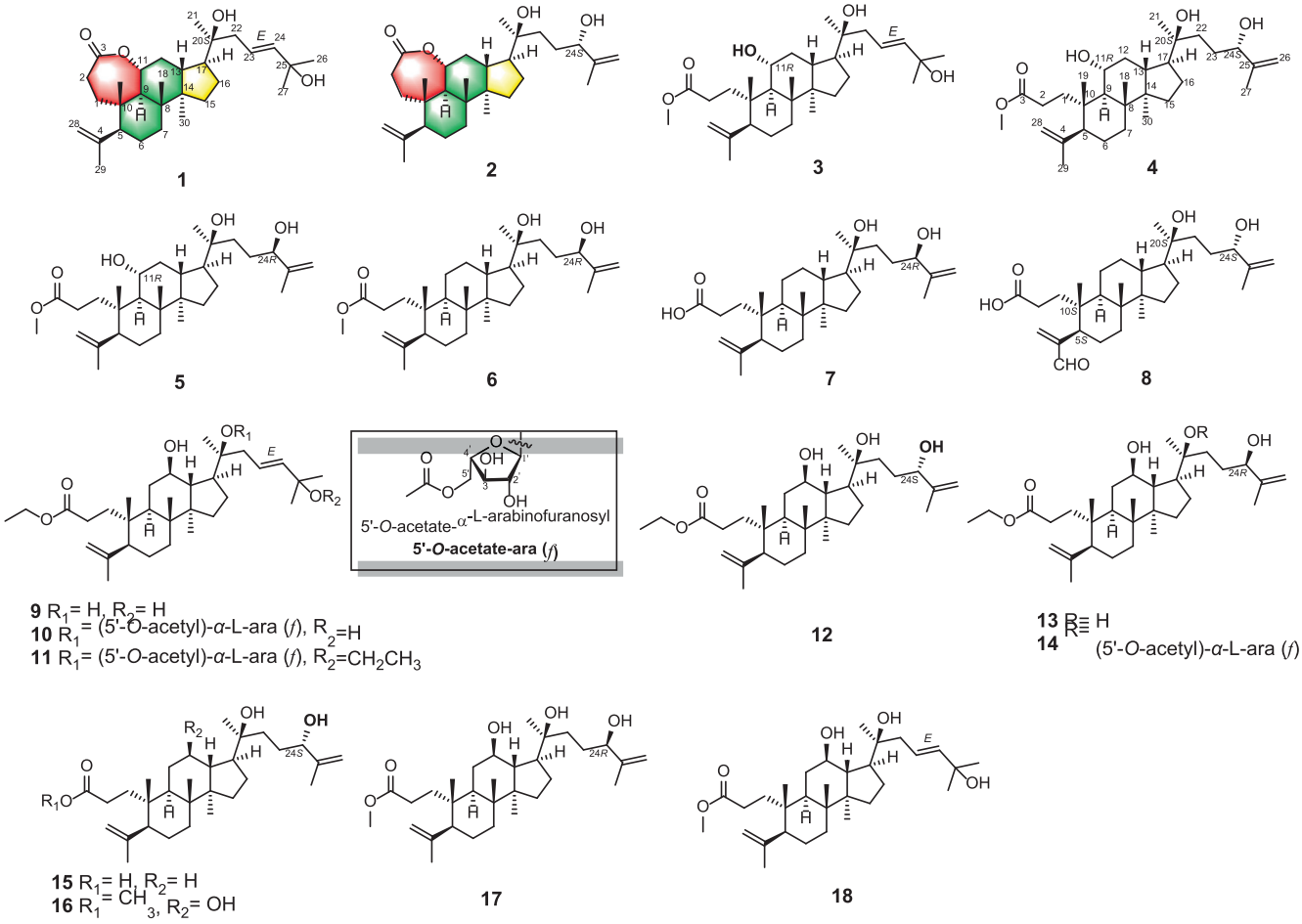

Fig. 1 Structure of compounds **1**–**18** isolated from Qingqianliu.

Agilent 1260 series semi preparative HPLC instrument (Agilent, Palo Alto, CA, USA) by using C18 columns (5 mm, 9.4 × 150 mm) with a flow rate of 2 mL/min. All analytical-grade solvents were bought from Merck KGaA (Darmstadt, Germany). Besides, chemical solvent were obtained from Shanghai Titan Scientific Co., ltd. P. R. China and silica gel (300–400 mesh) for column chromatographic were purchased from Qingdao Marine Chemical Inc. P. R. China. Similarly, Sephadex LH-20 gel were bought from GE Health care, Sweden and Lichrospher RP-18 gel (20–45 μm) from Merck KGaA (Darmstadt, Germany).

2.2. Plant material

The leaves of *Cyclocarya paliurus* (Batalin) Iljinskaja were purchased from Huaihua, Hunan Province, People's Republic of China, in June 2015, and authenticated by Prof. Wei Wang of Hunan University of Chinese Medicine. The voucher specimen (No. 20150629) was preserved in the TCM and Ethnomedicine Innovation & Development Laboratory, School of Pharmacy, Hunan University of Chinese Medicine, People′s Republic of China.

2.3. Extraction and isolation

The crude extract (4 Kg) was extracted from Qingqianliu (20.0 Kg) using 95 % ethanol percolation for three times at room temperature. Afterwards, the ethanol extract was suspended in water and then extracted with petroleum ether (PE), chloroform ($CHCl_3$), and *n*-butanol (*n*-BuOH) respectively. The chloroform layer (980.0 g) was subjected to silica gel column (60 × 15.5 cm) chromatography eluted with CH_2Cl_2-CH_3OH (0:1–1:1) to gain nineteen fractions (Fr. E1-E19). Fraction E7 (5.2 g) was purified using silica gel column (60 × 15.5 cm) chromatography eluted with CYH-EA (0:1–1:1) and reverse-phase HPLC (2.0 mL/min, MeCN-H_2O, 7.0:3.0) afforded **10** (4.0 mg) and **14** (4.0 mg). Combined fractions E8 and E9 named fractions E8-9 (33.9 g), which through silica gel column with PE-EA (0:1–1:1) to give thirteen fractions (Fr. F1-F13). Sub fraction F9 (2.5 g) through silica gel column chromatography yield **1** (12.5 mg), **2** (7.0 mg), **3** (15.2 mg), **4** (5.8 mg), **5** (4.1 mg), **11** (4.4 mg), **12** (27.4 mg), and **13** (32.4 mg). Similarly, fraction F10 (4.6 g) was subjected using Sephadex LH-20 column (4 × 77 cm) chromatography eluted with CH_3OH and reverse-phase HPLC (2.0 mL/min, MeCN-0.01 % F_3CCOOH-H_2O, 6.5:3.5) to produce **6** (9.1 mg), **7** (4.4 mg), **8** (3.8 mg), **9** (17.9 mg), **15** (4.0 mg), and **18** (8.2 mg). Compounds **16** (5.2 mg) and **17** (4.2 mg) were separated from fraction E13 (10.0 g) *via* silica gel column (60 × 15.5 cm) chromatography eluted with CYH-EA (0:1–1:1) and purified by reverse-phase HPLC (2.0 mL/min, MeCN-H_2O, 7.0:3.0).

2.3.1. Qingqianliusu A (1)

Colorless cubic crystal; mp 169 ~ 171℃; [α]23 D = + 67.0 (*c* 0.19, MeOH); UV (MeOH) λ^{max} (log ε): 204 (3.93) nm; IR (ν_{max}): 3369, 2950, 2959, 2930, 2907, 1728 cm^{-1}; ^1H and ^{13}C NMR (CD_3OD, Tables 1 and 2); HR-ESI-MS *m*/*z* 495.3450 $[M + Na]^+$ (calcd. for $C_{30}H_{48}O_4Na$, 495.3450).

2.3.2. Qingqianliusu B (2)

Colorless amorphous powder; [α]23 D = + 76.0 (*c* 0.25, MeOH); UV (MeOH) λ^{max} (log ε): 203 (3.71) nm; IR (ν_{max}): 3407, 2944, 2873, 1709 cm^{-1}; ^1H and ^{13}C NMR (CD_3OD, Tables 1 and 2); HR-ESI-MS *m*/*z* 495.3451 $[M + Na]^+$ (calcd. for $C_{30}H_{48}O_4Na$, 495.3450).

2.3.3. Qingqianliusu C (3)

Colorless powder; [α]23 D = + 38.5 (*c* 0.29, MeOH); UV (MeOH) λ^{max} (log ε): 204 (3.91) nm; IR (ν_{max}): 3408, 2963, 2871, 1717 cm^{-1}; ^1H and ^{13}C NMR (CD_3OD, Tables 1 and 2); HR-ESI-MS *m*/*z* 527.3712 $[M + Na]^+$ (calcd. for $C_{31}H_{52}O_5Na$, 527.3712).

2.3.4. Qingqianliusu D (4)

Colorless amorphous powder; [α]23 D = + 36.0 (*c* 0.25, MeOH); UV (MeOH) λ^{max} (log ε): 203 (3.84) nm; IR (ν_{max}): 3358, 2944, 2878, 1732 cm^{-1}; ^1H and ^{13}C NMR (CD_3OD, Tables 1 and 2); HR-ESI-MS *m*/*z* 527.3719 $[M + Na]^+$ (calcd. for $C_{31}H_{52}O_5Na$, 527.3712).

2.3.5. Qingqianliusu E (5)

White amorphous powder; [α]23 D = + 39.4 (*c* 0.33, MeOH); UV (MeOH) λ^{max} (log ε): 203 (3.81) nm; IR (ν_{max}): 3269, 2940, 2868, 1734 cm^{-1}; ^1H and ^{13}C NMR (CD_3OD, Tables 1 and 2); HR-ESI-MS *m*/*z* 527.3717 $[M + Na]^+$ (calcd. for $C_{31}H_{52}O_5Na$, 527.3712).

2.3.6. Qingqianliusu F (6)

White amorphous powder; [α]23 D = + 39.9 (*c* 0.28, MeOH). UV (MeOH) λ^{max} (log ε): 204 (4.00) nm; IR (ν_{max}): 3364, 2950, 2943, 2868, 1732 cm^{-1}; ^1H and ^{13}C NMR (CD_3OD, Tables 1 and 2); HR-ESI-MS *m*/*z* 511.3764 $[M + Na]^+$ (calcd. for $C_{31}H_{52}O_4Na$, 511.3763).

2.3.7. Qingqianliusu G (7)

White amorphous powder; [α]23 D = + 36.0 (*c* 0.22, MeOH); UV (MeOH) λ^{max} (log ε): 203 (3.69) nm; IR (ν_{max}): 3388, 2949, 2869, 1712 cm^{-1}; ^1H and ^{13}C NMR (CD_3OD, Tables 1 and 2); HR-ESI-MS *m*/*z* 497.3589 $[M + Na]^+$ (calcd. for $C_{30}H_{50}O_4Na$, 497.3607).

2.3.8. Qingqianliusu H (8)

White amorphous powder; [α]23 D = + 14.3 (*c* 0.21, MeOH); UV (MeOH) λ^{max} (log ε): 204 (3.76) nm; IR (ν_{max}): 3432, 2937, 2868, 1708, 1692 cm^{-1}; ^1H and ^{13}C NMR (CD_3OD, Tables 1 and 2); HR-ESI-MS *m*/*z* 511.3382 $[M + Na]^+$ (calcd. for $C_{30}H_{48}O_5Na$, 511.3399).

2.3.9. Qingqianliusu I (9)

Colorless amorphous powder; [α]23 D = + 33.2 (*c* 0.21, MeOH); UV (MeOH) λ^{max} (log ε): 204 (3.89) nm; IR (ν_{max}): 3259, 2949, 2875, 1735 cm^{-1}. ^1H and ^{13}C NMR (CD_3OD, Tables 1 and 2); HR-ESI-MS *m*/*z* 541.3869 $[M + Na]^+$ (calcd. for $C_{32}H_{54}O_5Na$, 541.3868).

2.3.10. Qingqianliusu J (10)

White amorphous powder; [α]23 D = + 7.2 (*c* 0.29, MeOH); UV (MeOH) λ^{max} (log ε): 204 (3.95) nm; IR (ν_{max}): 3351, 2927,

Table 1 ^{1}H spectroscopic data of compounds **1**–**14** (in CD_3OD, *J* in Hz at 600 MHz).

No.	1	2	3	4	5	6	7	8	9	10	11	12	13	14
1a	1.78 (m)	1.78 (m)	2.35 (m)	2.35 (m)	2.35 (m)	1.61 (m)	1.61 (m)	1.49 (m)	1.62 (m, 2H)	1.63 (m, 2H)	1.63 (m, 2H)	1.63 (m, 2H)	1.63 (m, 2H)	1.63 (m, 2H)
1b	1.33 (*t*-like, 13.5)	1.32 (*t*-like, 13.5)	1.54 (m)	1.56 (m)	1.55 (m)	1.59 (m)	1.59 (m)	0.86 (m)						
2a	2.81 (dd, 15.4, 12.7)	2.81 (dd, 15.7, 12.4)	2.64 (m)	2.64 (m)	2.63 (m)	2.39 (m)	2.34 (m)	2.59 (ddd, 16.0, 12.1, 4.0)	2.38 (m)	2.37 (m)	2.38 (m)	2.38 (m)	2.38 (m)	2.38 (m)
2b	2.30 (dd, 15.4, 8.1)	2.30 (dd, 15.4, 8.1)	2.33 (m)	2.34 (m)	2.34 (m)	2.21 (m)	2.15 (m)	2.12 (ddd, 16.0, 12.1, 5.5)	2.21 (m)	2.20 (m)	2.21 (m)	2.20 (m)	2.20 (m)	2.21 (m)
5	1.87 (m)	1.87 (m)	2.07 (dd, 12.9, 3.4)	2.07 (dd, 12.1, 4.1)	2.07 (dd, 12.8, 3.4)	2.05 (dd, 12.8, 3.2)	2.05 (dd, 12.7, 3.1)	2.74 (dd, 13.2, 3.2)	2.05 (m)	2.05 (m)	2.06 (m)	2.06 (m)	2.06 (m)	2.05 (m)
6a	2.02 (qd, 13.2, 4.0)	2.00 (qd, 13.3, 3.9)	1.88 (m)	1.88 (m)	1.87 (m)	1.90 (m)	1.88 (m)	1.98 (dd, 13.2, 3.2)	1.91 (m)	1.91 (m)	1.92 (m)	1.91 (m)	1.91 (m)	1.93 (m)
6b	1.44 (m)	1.43 (m)	1.33 (m)	1.32 (m)	1.32 (m)	1.36 (m)	1.35 (m)	1.23 (m)	1.39 (m)	1.40 (m)	1.40 (m)	1.39 (m)	1.39 (m)	1.40 (m)
7a	1.65 (m)	1.66 (m)	1.57 (m)	1.57 (m)	1.56 (m)	1.61 (m)	1.62 (m)	1.62 (m)	1.60 (m)	1.61 (m)	1.61 (m)	1.59 (m)	1.60 (m)	1.61 (m)
7b	1.23 (m)	1.23 (m)	1.20 (m)	1.19 (m)	1.19 (m)	1.25 (m)	1.24 (m)	1.24 (m)	1.28 (m)	1.27 (m)	1.26 (m)	1.27 (m)	1.27 (m)	1.27 (m)
9	1.84 (d, 9.6)	1.84 (d, 9.7)	1.73 (m)	1.73 (m)	1.74 (m)	1.60 (m)	1.61 (m)	1.70 (m)	1.68 (dd, 13.4, 2.9)	1.66 (dd, 13.5, 3.1)	1.66 (dd, 13.6, 3.1)	1.67 (dd, 13.2, 3.2)	1.66 (d, 13.3, 3.1)	1.66 (m)
11a	4.78 (q-like, 8.8)	4.78 (q-like, 8.8)	3.92 (td, 10.8, 5.0)	3.91 (td, 10.9, 5.0)	3.91 (td, 10.8, 5.0)	1.44 (m)	1.46 (m)	1.44 (m)	1.77 (m)	1.74 (m)	1.75 (m)	1.76 (m)	1.75 (m)	1.76 (m)
11b						1.36 (m)	1.33 (m)	1.32 (m)	1.33 (m)	1.31 (m)	1.29 (m)	1.31 (m)	1.30 (m)	1.32 (m)
12a	2.47 (ddd, 13.8, 8.0, 4.5)	2.46 (ddd, 13.8, 7.9, 4.5)	2.13 (m)	2.12 (m)	2.12 (m)	1.89 (m)	1.88 (m)	1.87 (m)	3.58 (td, 10.6, 5.1)	3.69 (td, 10.4, 5.3)	3.71 (td, 10.5, 5.3)	3.56 (td, 10.6, 5.1)	3.57 (td, 10.6, 5.1)	3.70 (td, 10.4, 5.3)
12b	1.68 (m)	1.68 (m)	1.45 (m)	1.46 (m)	1.46 (m)	1.30 (m)	1.31 (m)	1.30 (m)	–	–	–	–	–	–
13	1.89 (m)	1.87 (m)	1.88 (m)	1.87 (m)	1.85 (m)	1.74 (m)	1.72 (m)	1.72 (m)	1.80 (m)	1.80 (m)	1.77 (m)	1.79 (m)	1.79 (m)	1.78 (m)
15a	1.54 (m)	1.52 (m)	1.41 (m)	1.41 (m)	1.41 (m)	1.49 (m)	1.49 (m)	1.47 (m)	1.56 (m)	1.59 (m)	1.58 (m)	1.55 (m)	1.53 (m)	1.59 (m)
15b	1.10 (m)	1.11 (m)	1.06 (m)	1.08 (m)	1.08 (m)	1.09 (m)	1.08 (m)	1.07 (m)	1.07 (m)	1.06 (m)	1.06 (m)	1.09 (m)	1.09 (m)	1.09 (m)
16a	1.80 (m)	1.79 (m)	1.75 (m)	1.74 (m)	1.75 (m)	1.75 (m)	1.74 (m)	1.73 (m)	1.88 (m)	1.87 (m)	1.90 (m)	1.88 (m)	1.88 (m)	1.91 (m)
16b	1.66 (m)	1.62 (m)	1.63 (m)	1.61 (m)	1.60 (m)	1.60 (m)	1.58 (m)	1.59 (m)	1.40 (m)	1.41 (m)	1.39 (m)	1.32 (m)	1.35 (m)	1.35 (m)
17	1.79 (m)	1.78 (m)	1.79 (m)	1.80 (m)	1.78 (m)	1.75 (m)	1.75 (m)	1.74 (m)	2.08 (m)	2.24 (m)	2.27 (m)	2.07 (m)	2.06 (m)	2.27 (m)
18	1.00 (s)	1.00 (s)	1.06 (s)	1.05 (s)	1.05 (s)	1.06 (s)	1.06 (s)	1.09 (s)	1.08 (s)	1.06 (s)	1.07 (s)	1.06 (s)	1.06 (s)	1.06 (s)
19	1.20 (s)	1.20 (s)	1.07 (s)	1.07 (s)	1.07 (s)	0.88 (s)	0.88 (s)	0.84 (s)	0.91 (s)	0.91 (s)	0.91 (s)	0.91 (s)	0.91 (s)	0.91 (s)
21	1.14 (s)	1.14 (s)	1.16 (s)	1.14 (s)	1.14 (s)	1.13 (s)	1.12 (s)	1.13 (s)	1.15 (s)	1.33 (s)	1.32 (s)	1.15 (s)	1.14 (s)	1.33 (s)
22a	2.20 (m)	1.50 (m)	2.21 (m)	1.54 (m)	1.58 (m)	1.59 (m)	1.58 (m)	1.50 (m)	2.32 (m)	2.54 (dd, 14.3, 5.6)	2.59 (dd, 14.2, 6.2)	1.53 (m)	1.54 (m)	1.75 (m)
22b	2.18 (m)	1.40 (m)	2.19 (m)	1.41 (m)	1.39 (m)	1.40 (m)	1.39 (m)	1.38 (m)	2.20 (m)	2.37 (m)	2.32 (m)	1.31 (m)	1.30 (m)	1.63 (m)
23a	5.67 (ddd, 15.6, 7.5, 6.2)	1.65 (m)	5.68 (ddd, 15.7, 7.5, 6.3)	1.64 (m)	1.65 (m)	1.65 (m)	1.64 (m)	1.61 (m)	5.74 (ddd, 15.7, 8.6, 6.0)	5.73 (ddd, 15.7, 8.0, 5.6)	5.74 (ddd, 15.8, 8.5, 6.1)	1.74 (m)	1.76 (m)	1.80 (m)
23b		1.57 (m)		1.55 (m)	1.55 (m)	1.57 (m)	1.56 (m)	1.58 (m)				1.57 (m)	1.54 (m)	1.53 (m)
24	5.62 (d, 15.6)	3.97 (t, 6.5)	5.63 (d, 15.7)	3.96 (t, 6.7)	3.98 (t, 6.1)	3.96 (t, 6.2)	3.96 (t, 6.2)	3.96 (t, 6.5)	5.63 (d, 15.7)	5.63 (d, 15.7)	5.55 (d, 15.8)	4.00 (t, 6.4)	3.98 (t, 5.9)	3.98 (t, 6.4)
26a	1.27 (s)	4.91 (br s)	1.28 (s)	4.91 (br	4.92 (br	4.92 (br	4.92 (br	4.91 (br s)	1.29 (s)	1.29 (s)	1.28 (s)	4.93 (br	4.93 (br	4.74 (br

Table 1 (*continued*)

No.	1	2	3	4	5	6	7	8	9	10	11	12	13	14
				s)	s)	s)	s)					s)	s)	s)
26b		4.81 (br s)		4.82 (br s)	4.81 (br s)	4.82 (br s)	4.81 (br s)	4.81 (br s)				4.82 (br s)	4.82 (br s)	4.71 (br s)
27	1.26 (s)	1.72 (s)	1.26 (s)	1.75 (s)	1.73 (s)	1.73 (s)	1.72 (s)	1.72 (s)	1.28 (s)	1.28 (s)	1.27 (s)	1.73 (s)	1.73 (s)	1.74 (s)
28a	4.86 (br s)	4.85 (br s)	4.85 (br s)	4.85 (br s)	4.85 (br s)	4.86 (br s)	4.86 (br s)	6.42 (br s)	4.88 (br s)	4.88 (br s)	4.88 (br s)	4.88 (br s)	4.88 (br s)	4.88 (br s)
28b	4.74 (br s)	4.74 (br s)	4.69 (br s)	4.69 (br s)	4.69 (br s)	4.69 (br s)	4.69 (br s)	6.22 (br s)	4.71 (br s)	4.71 (br s)	4.71 (br s)	4.71 (br s)	4.71 (br s)	4.71 (br s)
29	1.75 (s)	1.75 (s)	1.75 (s)	1.76 (s)	1.75 (s)	1.75 (s)	1.75 (s)	9.44 (s)	1.76 (s)	1.77 (s)	1.76 (s)	1.76 (s)	1.77 (s)	1.76 (s)
30	0.97 (s)	0.97 (s)	0.97 (s)	0.97 (s)	0.96 (s)	0.94 (s)	0.95 (s)	0.98 (s)	0.95 (s)	0.95 (s)	0.96 (s)	0.95 (s)	0.96 (s)	0.97 (s)
3-COO*CH*$_3$	\	\	3.63 (s)	3.62 (s)	3.62 (s)	3.66 (s)								
3-COO*CH*$_2$*C*H$_3$									4.11 (q, 7.1)	4.11 (q, 7.1)	4.12 (q, 7.1)	4.11 (q, 7.1)	4.11 (q, 7.2)	4.11 (q, 7.1)
3-COOCH$_2$*CH*$_3$									1.24 (t, 7.1)	1.25 (t, 7.1)	1.25 (t, 7.1)	1.25 (t, 7.1)	1.25 (t, 7.2)	1.25 (t, 7.1)
1′										5.27 (d, 2.9)	5.27 (d, 2.9)			5.27 (d, 2.8)
2′										3.94 (dd, 4.9, 2.9)	3.95 (dd, 4.8, 2.9)			3.96 (dd, 4.8, 2.8)
3′										3.82 (dd, 6.4, 4.9)	3.82 (dd, 6.3, 4.8)			3.82 (dd, 6.6, 4.8)
4′										4.11 (m)	4.10 (m)			4.07 (m)
5′a										4.26 (m)	4.26 (m)			4.26 (m)
5′b										4.13 (m)	4.11 (m)			4.13 (m)
5′-OCO*CH*$_3$										2.06 (s)	2.06 (s)			2.06 (s)
25-O*CH*$_2$CH$_3$											3.39 (q, 7.0)			
25-OCH$_2$*CH*$_3$											1.12 (t, 7.0)			

Table 2 ^{13}C spectroscopic data of compounds **1**–**14** (in CD_3OD, *J* in Hz at 600 MHz).

No.	1	2	3	4	5	6	7	8	9	10	11	12	13	14
1	40.6t	40.6,t	31.7t	37.7t	37.7t	35.9t	36.0t	36.2t	35.8t	35.8t	35.8t	35.8t	35.8t	35.7t
2	30.5t	30.5t	30.2t	30.3t	30.2t	29.4t	29.4t	28.8t	29.6t	29.7t	29.7t	29.6t	29.6t	29.6t
3	179.6s	179.6s	177.3s	177.3s	177.3s	176.4s	178.2s	178.0s	175.8s	175.7s	175.8s	175.7s	175.7s	175.7s
4	148.3s	148.3s	149.1s	149.1s	149.1s	148.9s	149.0s	154.2s	148.7s	148.7s	148.7s	148.6s	148.6s	148.7s
5	58.7 d	58.7 d	52.8 d	52.8 d	52.8 d	52.0 d	52.0 d	40.2 d	51.7 d	51.7 d	51.7 d	51.7 d	51.7 d	51.7 d
6	26.3t	26.3t	26.1t	26.1t	26.1t	25.9t	25.9t	26.3t	25.8t	25.8t	25.8t	25.8t	25.8t	25.8t
7	34.7t	34.7t	35.8t	35.8t	35.8t	35.1t	35.1t	35.2t	34.6t	34.5t	34.5t	34.6t	34.6t	34.5t
8	41.8s	41.8s	41.7s	41.6s	41.6s	41.3s	41.3s	41.3s	40.6s	40.7s	40.7s	40.6s	40.6s	40.6s
9	53.5 d	53.5 d	46.4 d	46.4 d	46.4 d	42.3 d	42.3 d	42.3 d	41.7 d	41.3 d	41.3 d	41.7 d	41.7 d	41.3 d
10	40.7s	40.7s	40.6s	40.6s	40.6s	40.2s	40.2s	39.5s	40.2s	40.2s	40.2s	40.2s	40.2s	40.2s
11	78.5 d	78.5 d	71.6 d	71.6 d	71.6 d	23.2t	23.2t	23.4t	32.5t	31.3t	31.3t	32.6t	32.6t	31.3t
12	37.0t	37.0t	40.1t	40.0t	40.0t	28.6t	28.6t	28.5t	71.8 d	71.5 d	71.4 d	71.7 d	71.7 d	71.3 d
13	39.9 d	40.0 d	42.0 d	42.0 d	42.0 d	43.6 d	43.6 d	43.6 d	49.3 d	50.0 d	50.0 d	49.0 d	49.0 d	49.6 d
14	51.0s	51.0s	51.6s	51.6s	51.6s	51.9s	51.9s	51.9s	53.1s	53.0s	53.0s	53.1s	53.1s	52.8s
15	31.6t	31.7t	31.8t	31.9t	31.9t	32.3t	32.3t	32.3t	32.0t	31.4t	31.4t	32.1t	32.1t	31.5t
16	25.8t	26.0t	25.7t	25.9t	25.9t	25.8t	25.8t	25.8t	27.2t	26.8t	26.9t	27.4t	27.4t	27.0t
17	51.9 d	52.4 d	50.3 d	50.5 d	50.8 d	51.0 d	51.1 d	50.8 d	54.5 d	52.7 d	52.6 d	55.0 d	55.1 d	52.8 d
18	17.5 q	17.4 q	16.9 q	16.8 q	16.8 q	15.8 q	15.8 q	15.8 q	16.1 q	16.2 q	16.2 q	15.9 q	16.0 q	16.1 q
19	19.3 q	19.4 q	21.3 q	21.1 q	21.1 q	20.8 q	20.8 q	19.6 q	20.7 q	20.6 q	20.6 q	20.8 q	20.8 q	20.6 q
20	75.7s	75.4s	75.9s	75.6s	75.6s	75.9s	75.9s	75.8s	74.5s	83.8s	83.7s	74.1s	74.3s	84.0s
21	26.1 q	25.5 q	26.0 q	25.5 q	25.4 q	25.2 q	25.2 q	25.4 q	27.1 q	23.3 q	23.3 q	26.7 q	26.7 q	22.7 q
22	45.2t	37.9t	45.4t	38.3t	38.3t	38.2t	38.2t	38.2t	40.3t	39.9t	39.8t	32.2t	32.3t	32.6t
23	123.7 d	30.1t	123.8 d	30.2t	30.3t	30.2t	30.2t	30.1t	124.1 d	123.5 d	126.9 d	30.0t	30.1t	30.4t
24	142.2 d	77.4 d	142.1 d	77.4 d	77.3 d	77.3 d	77.3 d	77.5 d	141.6 d	142.0 d	139.6 d	77.4 d	77.4 d	77.2 d
25	71.2s	148.8s	71.2s	148.8s	149.0s	149.0s	149.0s	148.8s	71.2s	71.2s	76.3s	148.8s	149.2s	149.3s
26	29.9 q	111.6t	29.9 q	111.6t	111.3t	111.3t	111.3t	111.6t	29.8 q	29.9 q	26.9 q	111.4t	111.1t	111.2t
27	30.0 q	17.5 q	30.0 q	17.5 q	17.8 q	17.8 q	17.8 q	17.5 q	30.0 q	30.0 q	26.9 q	17.7 q	17.9 q	18.0 q
28	114.6t	114.6t	114.2t	114.2t	114.2t	114.0t	113.9t	138.3t	114.6t	114.2t	114.2t	114.2t	114.2t	114.2t
29	23.9 q	23.8 q	23.8 q	23.8 q	23.8 q	23.7 q	23.7 q	196.6 d	23.7 q	23.7 q	23.7 q	23.7 q	23.7 q	23.7 q
30	16.1 q	16.1 q	16.6 q	16.7 q	16.7 q	16.9 q	16.9 q	16.9 q	17.0 q	17.2 q	17.2 q	17.1 q	17.1 q	17.3 q
3-COO*CH*$_3$			51.9 q	51.9 q	51.9 q	52.1 q								
3-COO*CH*$_2$CH$_3$									61.6t	61.6t	61.6t	61.6t	61.6t	61.6t
3-COOCH$_2$*CH*$_3$									14.5 q	14.5 q	14.5 q	14.5 q	14.5 q	14.5 q
1′-O*CH*-										103.5 d	103.6 d			103.4 d
2′-*CH*-										83.7 d	83.6 d			83.5 d
3′-*CH*-										77.9 d	78.0 d			78.1 d
4′-*CH*-										82.1 d	82.2 d			82 d
5′-*CH*$_2$-*O*										65.2t	65.3t			65.3t
5′-O*CO*-										172.6s	172.6s			172.6s
5′-OCO*CH*$_3$										20.7 q	20.7 q			20.7 q
25-O*CH*$_2$CH$_3$											59.0t			
25-OCH$_2$*CH*$_3$											16.4 q			

1734 cm^{-1}; ^1H and ^{13}C NMR (CD_3OD, Tables 1 and 2); HR-ESI-MS *m*/*z* 715.4400 $[M + Na]^+$ (calcd. for $C_{39}H_{64}O_{10}Na$, 715.4397).

2.3.11. Qingqianliusu K (*11*)

White amorphous powder; [α]23 D = + 12.0 (*c* 0.25, MeOH); UV (MeOH) λ^{max} (log ε): 204 (3.82) nm; IR (ν_{max}): 3401, 2973, 1734 cm^{-1}. ^1H and ^{13}C NMR (CD_3OD, Tables 1 and 2); HR-ESI-MS *m*/*z* 743.4718 $[M + Na]^+$ (calcd. for $C_{41}H_{68}O_{10}Na$, 743.4710).

2.3.12. Qingqianliusu L (*12*)

White amorphous powder; [α]23 D = + 24.2 (*c* 0.41, MeOH); UV (MeOH) λ^{max} (log ε): 204 (3.94) nm; IR (ν_{max}): 3292, 2942, 2872, 1733 cm^{-1}. ^1H and ^{13}C NMR (CD_3OD, Tables 1 and 2); HR-ESI-MS *m*/*z* 541.3863 $[M + Na]^+$(calcd. for $C_{32}H_{54}O_5$-Na, 541.3869).

2.3.13. Qingqianliusu M (*13*)

White amorphous powder; [α]23 D = + 40.8 (*c* 0.59, MeOH); UV (MeOH) λ^{max} (log ε): 204 (3.77) nm; IR (ν_{max}): 3265, 2941, 2875, 1732 cm^{-1}. ^1H and ^{13}C NMR (CD_3OD, Tables 1 and 2); HR-ESI-MS *m*/*z* 541.3859 $[M + Na]^+$(calcd. for $C_{32}H_{54}O_5$-Na, 541.3869).

2.3.14. Qingqianliusu N (*14*)

White amorphous powder; [α]23 D = + 7.2 (*c* 0.28, MeOH); UV (MeOH) λ^{max} (log ε): 203 (3.77) nm; IR (ν_{max}): 3287, 2916,

2849, 1728 cm^{-1}. ^{1}H and ^{13}C NMR (CD_3OD, Tables 1 and 2); HR-ESI-MS *m/z* 715.4382 $[M + Na]^+$ (calcd. for $C_{39}H_{64}O_{10}$-Na, 715.4397).

2.4. Determination of the absolute configurations of the Sugars

The acid hydrolysis was adopted from reported method (Liu et al., 2020; Shen et al., 2020). After the comparison of the retention times (t_R) of monosaccharide derivatives with those of standard products: L-Arabinose (19.75 min) and D-Arabinose (23.96 min), compounds **10**, **11**, and **14** were determined to be L-Arabinose. Detailed description of the procedure can be seen in the Supporting Information (**Text S1.**).

2.5. X-ray crystallographic Analysis

All data were obtained using a SuperNova, AtlasS2 diffractometer with graphite monochromated Cu Ka radiation (λ = 1.54184 Å). The structure was solved by direct method with the SHELXTL software package and was refined by full-matrix least-squares techniques. All the nonhydrogen atoms were refined anisotropically and H atoms were located in geometrical calculations. Crystal data for compounds **1** and **18** were listed below.

2.5.1. Crystal data for *1*

CCDC: 2133487, $C_{30}H_{48}O_4$, M = 472.68 g/mol, monoclinic space group $P2_1$, a = 14.0820(8) Å, b = 8.2422(3) Å, c = 24.0159(11) Å, β = 100.684(5)°, V = 2739.1(2) $Å^3$, Z = 4, T = 149.99(10) K, μ(Cu Kα) = 0.576 mm^{-1}, $Dcalc$ = 1.146 g/cm^3, 21,646 reflections measured ($6.388 \leq 2\Theta \leq 150.052$), 9167 unique ($R_{int}$ = 0.0538, R_{sigma} = 0.0530) which were used in all calculations. The final R_1 was 0.0781 ($I > 2\sigma(I)$) and wR_2 was 0.2170. Flack parameter = − 0.3(2).

2.5.2. Crystal data for *18*

CCDC: 2133486, $C_{31}H_{52}O_5$, M = 504.72 g/mol, tetragonal space group $P4_12_12$, a = 19.3567(2) Å, c = 16.0224(3) Å, V = 6003.30(17) $Å^3$, Z = 8, T = 149.99(10) K, μ(Cu Kα) = 0.578 mm^{-1}, $Dcalc$ = 1.117 g/cm^3, 32,912 reflections measured ($6.458 \leq 2\Theta \leq 133.17$), 5302 unique ($R_{int}$ = 0.0326, R_{sigma} = 0.0186) which were used in all calculations. The final R_1 was 0.0626 ($I > 2\sigma(I)$) and wR_2 was 0.1679. Flack parameter = -0.05(6).

2.6. α-Glucosidase inhibitory activity Assay

The α-glucosidase inhibition assay was adopted from reported method (Perez et al., 2019; Smirnova et al., 2020; Zhou et al., 2021). The detailed protocol was described in the Supporting Information (**Text 2**).

2.7. Anti-inflammatory activity against COX-2

The COX-2 inhibition assay was detected with previous report (Chai et al., 2008; Shataer et al., 2021). The detailed procedures for this assay were discussed in the Supporting Information (**Text 3**).

2.8. Cytotoxic Bioassays

Using the previously described MTT method (Chen et al., 2018; Gao et al., 2016; Peng et al., 2019; Sun et al., 2021; Yan et al., 2014; Zhou et al., 2021), the cytotoxicities of new compounds against the human cancer cell lines (BGC-823, MCF-7, HCT-116, and HepG-2) were measured. Paclitaxel was used as positive control. The detailed process can be seen in the Supporting Information (**Text 4**).

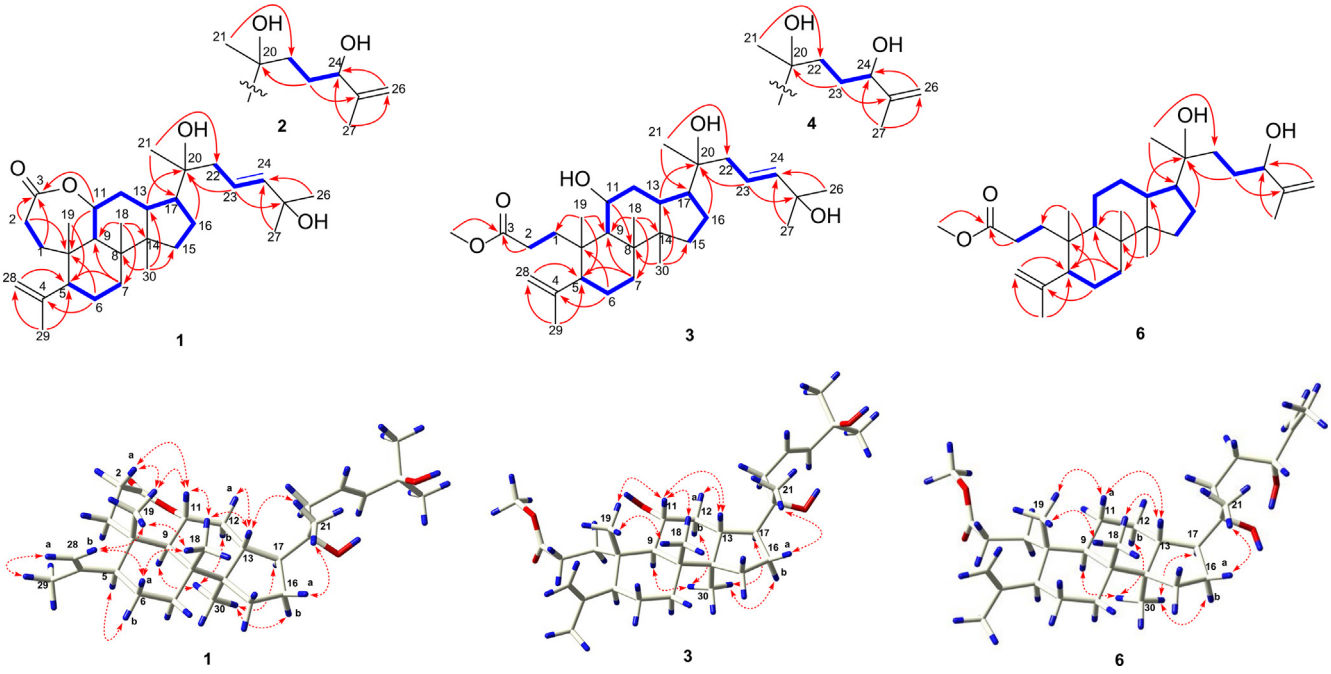

Fig. 2 Key ^{1}H–^{1}H COSY (blue thick bonds) and HMBC (red solid arrows) correlations of compounds **1**–**4**, and **6**, together with NOESY (red dash arrows) correlations of compounds **1**, **3**, and **6.**

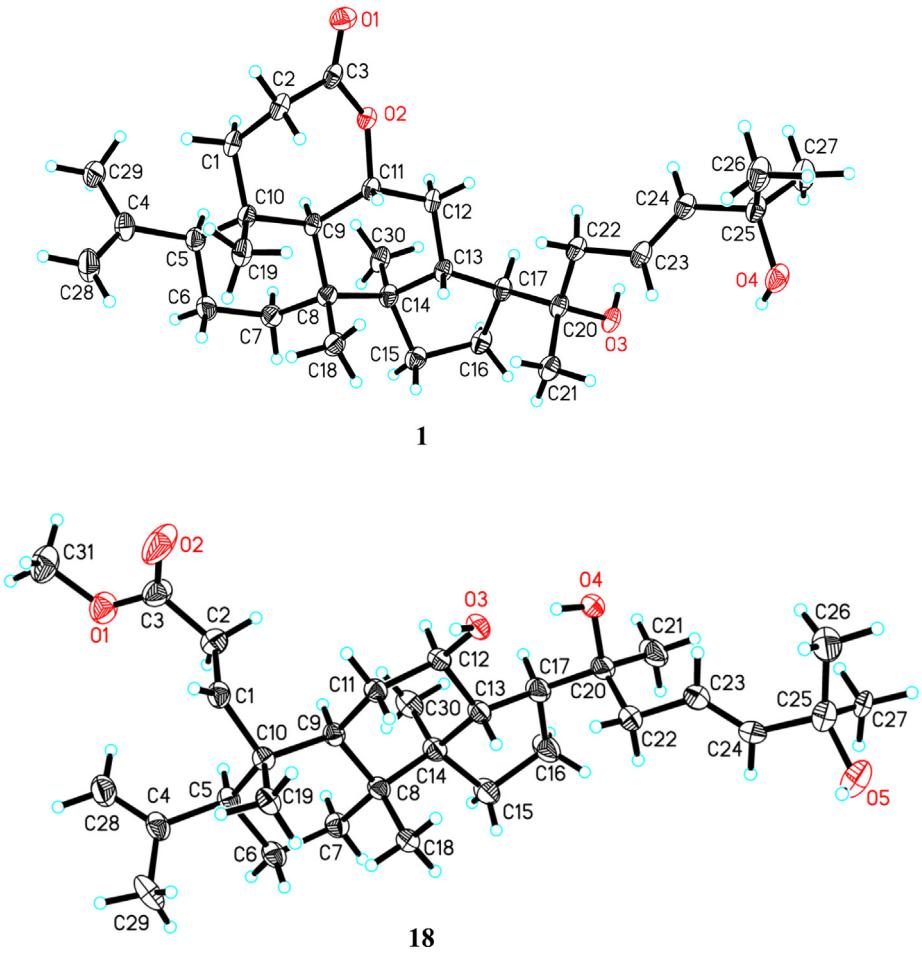

Fig. 3 Crystal structures of compounds **1**, and **18**.

3. Results and discussion

3.1. Structure Determination

The chloroform extract of Qingqianliu was isolated and fractionated over Sephadex LH-20, silica gel, RP-18 (ODS), and semi-preparative HPLC to obtain fourteen undiscovered compounds named Qingqianliusus A-N (**1**–**14**), as well as four reported compounds, 20*S*,24*S*-dihydroxy-3,4-*seco*-dammara-4 (28),25-dien,3-oic acid (**15**) (Aoki et al., 1988), cyclocariol B (**16**) (Chen et al., 2018), cyclocariol A (**17**) (Chen et al., 2018), and cyclocariol E (**18**) (Chen et al., 2018). In addition, compound **15** was reported from Qingqianliu for the first time.

Qingqianliusu A (**1**), an optical rotation value of [α]23 D = + 67.0 (*c* 0.19, MeOH), was obtained as cubic crystals (CH_3-CN-CH_3OH) with mp 169 ∼ 171℃. The molecular formula $C_{30}H_{48}O_4$ was established by $[M + Na]^+$ ion at *m*/*z* 495.3450 (calcd. for $C_{30}H_{48}O_4Na$, 495.3450) in HR-ESI-MS (**Fig. S6**). Its IR spectrum (**Fig. S8**) revealed characteristic absorption peaks for hydroxyl (3369 cm^{-1}), methyl (2950, 2930, 1457, 1387 cm^{-1}), double bond (1644 cm^{-1}), and carbonyl groups (1728 cm^{-1}). The ^1H NMR data (Table 1) exhibited resonances for four olefinic proton singlets at δ_H 5.67 (ddd, *J* = 15.6, 7.5, 6.2 Hz, H-23), 5.62 (d, *J* = 15.6 Hz, H-24), 4.86 (br s, H-28a), and 4.74 (br s, H-28b); one oxygenated methine at δ_H 4.78 (q-like, *J* = 8.8 Hz, H-11); as well as seven methyl singlets at δ_H 1.75 (s, H_3-29), 1.26 (s, H_3-27), 1.27 (s, H_3-26), 1.20 (s, H_3-19), 1.14 (s, H_3-21), 1.00 (s, H_3-18), and 0.97 (s, H_3-30). According to the ^{13}C NMR (Table 2), DEPT-135°, and HSQC spectra (**Fig. S12**), 30 carbon signals including one carbonyl at δ_C 179.6 (C-3); four olefinic carbons at δ_C 148.3 (C-4), 142.2 (C-24), 123.7 (C-23), and 114.6 (C-28); one oxygenated sp^3 methine at δ_C 78.5 (C-11); five sp^3 quaternary carbons at δ_C 75.7 (C-20), 71.2 (C-25), 51.0 (C-14), 41.8 (C-8), and 40.7 (C-10); seven methyls at δ_C 29.9 (C-26), 30.0 (C-27), 26.1 (C-21), 23.9 (C-29), 19.3 (C-19), 17.4 (C-18), and 16.1 (C-30); as well as eight sp^3 methylenes at δ_C 45.2 (C-22), 40.6 (C-1), 37.0 (C-12), 34.7 (C-7), 31.6 (C-15), 30.5 (C-2), 26.3 (C-6), and 25.8 (C-16) were determined. All the above data indicated that **1** possessed a 3,4-*seco*-dammarane triterpenoid skeleton.

The ^1H–^1H COSY correlations (Fig. 2) of **1** demonstrated the presence of four spin-coupling systems (C-1 to C-2, C-5 to C-7, C-9 to C-15, C-22 to C-24). The HMBC spectrum (**Fig. S13**) showed the correlations from δ_H 4.78 (H-11) to δ_C 179.6 (C-3)/40.7 (C-10), δ_H 2.81 (H-2a)/2.30 (H-2b) to δ_C 40.7 (C-10), as well as δ_H 1.78 (H-1a)/1.33 (H-1b) to δ_C 179.6 (C-3), suggesting the existence of a 3,11-heptacyclic lactone unit, which was supported by the down-field shift of the resonance with δ_H 4.78 (q-like, *J* = 8.8 Hz, H-11). The correlations from δ_H 5.67 (H-23) to δ_C 75.7 (C-20)/71.2 (C-25), δ_H

1.26 (H-26)/1.27 (H-27) to δ_C 142.2 (C-24), δ_H 1.14 (H-21) to δ_C 51.9 (C-17)/45.2 (C-22) and δ_H 1.89 (H-13)/1.80 (H-16a) to δ_C 75.7 (C-20) showed that an eight-carbon side chain containing a double bond was attached to C-17. The configuration of the Δ^{23} double bond was *E* geometry due to the large coupling constant ($^3J_{H\text{-}23/H\text{-}24}$ = 15.6 Hz). In addition, the correlations of δ_H 1.75 (H-29) to δ_C 114.6 (C-28)/58.7 (C-5), δ_H 4.86 (H-28a)/4.74 (H-28b) to δ_C 58.7 (C-5), δ_H 1.00 (H_3-18) to δ_C 34.7 (C-7)/53.5 (C-9) /51.0 (C-14), δ_H 1.00 (H_3-30) to δ_C 41.8 (C-8)/39.9 (C-13) /31.6 (C-15), implied the planar structure of **1** (Fig. 2). The relative configuration of **1** were determined by ROESY spectrum (**Fig. S14**), in which the correlations of δ_H 1.87 (H-5)/1.84 (H-9)/1.79 (H-17)/0.97 (H_3-30) revealed that H-5, H-9, H-17, and H_3-30 were cofacial and randomly allocated to be α-oriented. Consequently, the *β*-orientations of H-11, H-13, H_3-18, and H_3-19 were defined by the ROESY cross-peaks of δ_H 4.78 (H-11)/1.89 (H-13)/1.00 (H_3-18)/1.20 (H_3-19). Furthermore, a single crystal X-ray diffraction analysis was thus successfully performed to expressly assign the stereochemistry of **1** (Fig. 3). The Flack parameter of −0.3 (2) could only allow the relative configuration of **1**. However, by analyzing several 3,4-*seco*-dammarane analogues (Aoki et al., 1988; Aoki et al., 1990; Chen et al., 2018; Phan et al., 2011; Takayuki and Toshifumi, 1979), as well as X-ray data (**Fig. S4**) of known analogue cyclocariol E (**18**) with a small Flack parameter of 0.05(6), it was found that the skeleton configurations of these compounds were stable. Therefore, based on the above evidence, the absolute structure of **1** was established as 23(*E*),11*R*,20*S*-11,20,25-trihydroxy-3,4-*seco*-dammara-4(28),23-dien-3 oic acid-3,11-heptacyclic lactone.

Qingqianliusu B (**2**) was obtained as a colorless amorphous powder with [α]23 D = + 76.0 (*c* 0.25, MeOH). The molecular formula, $C_{30}H_{48}O_4$, was based on its sodium adduct molecular ion $[M + Na]^+$ at *m/z* 495.3451 (calcd. for $C_{30}H_{48}O_4Na$, 495.3450) in HR-ESI-MS spectrum (**Fig. S15**). Comparison of the NMR data (Tables 1 and 2) of **2** with compound **1** suggested that they share a similar skeleton with the same 3,11-heptacyclic lactone unit. The only difference between **1** and **2** were at the eight-carbon side chain. Terminal double bond with chemical shift at δ_H 4.91 (H-26a)/4.81 (H-26b), δ_C 148.8 (C-25) and 111.6 (C-26) in **2** replaced *E*-type disubstituted double bond in **1**. Compound **2** also included one quaternary oxygen-bearing carbon at δ_C 75.4 (C-20), together with one oxygenated methine at δ_C 77.4 (C-24). The key HMBC correlations (**Fig. S22**) from δ_H 4.91 (H-26a)/4.81 (H-26b)/1.72 (H_3-27) to δ_C 77.4 (C-24), δ_H 1.65 (H-23a)/1.57 (H-23b) to δ_C 148.8 (C-25)/75.4 (C-20), and δ_H 1.14 (H-21) to δ_C 52.4 (C-17)/37.9 (C-22) revealed eight carbon side chain structure of **2**. Notably, the absolute configuration of chiral center (C-24) on the branch chain was determined by summarizing NMR data characteristics of epimers with *R*/*S* configuration at C-24 and single crystal data of corresponding compound cyclocariol B (**16**) (Chen et al., 2018). Please see "*3.3. Determination of the Absolute Configurations of Epimers*" of this article for more details. Thus, the structure of **2** was assigned as 23(*E*),11*R*,20*S*,24*S*-11,20,24-trihydroxy-3,4-*seco*-dammara-4(28),25-dien-3 oic acid-3,11-heptacyclic lactone.

Qingqianliusu C (**3**), a colorless powder with [α]23 D = + 38.5 (*c* 0.29, MeOH), had a molecular formula $C_{31}H_{52}O_5$ as determined by HR-ESI-MS on its sodium adduct molecular ion $[M + Na]^+$ at *m/z* 527.3712 (calcd. for $C_{31}H_{52}O_5Na$, 527.3712) (**Fig. S24**). In the ^{13}C NMR spectrum (**Fig. S28**), singlets were exhibited for four oxygenated carbon singlets at *δ* 75.9 (C-20), 71.6 (C-11), 71.2 (C-25), and 51.9 (3-COO$\underline{CH_3}$). The ^1H and ^{13}C NMR data (Tables 1 and 2) of **3** were analogous to those of cyclocariol E (**18**) (Chen et al., 2018), illustrating that **3** had similar 3,4-*seco*-dammarane skeleton with cyclocariol E. Moreover, in the HMBC spectrum (Fig. 2 **and Fig. S31**), key correlations from δ_H 3.63 (s, 3-COO$\underline{CH_3}$) to δ_C 177.3 (C-3) showed that a methoxy group was connected to the carbonyl. The correlations from δ_H 3.92 (td, *J* = 10.8, 5.0 Hz, H-11) to δ_C 41.7 (C-8) and 40.6 (C-10) verified the hydroxyl was located at C-11 in **3**, while one hydroxyl located at C-12 in cyclocariol E (**18**). The α-orientations of H-5, H-9, H-17, and H_3-30 were further to confirm with the ROESY correlations (Fig. 2 **and Fig. S32**) of δ_H 2.07 (H-5)/1.73 (H-9)/1.79 (H_3-17)/0.97 (H_3-30). Then, key correlations of δ_H 3.92 (H-11)/1.87 (H-13) /1.00 (H_3-18)/1.20 (H_3-19) suggested that H-11, H-13, H_3-18, and H_3-19 are *β*-oriented. Thus, the configuration of C-11 in **3** was proved as S by comparing with the structure and ROESY correlation (Fig. 2) of **1**. Accordingly, the compound **3** was determined as 23(*E*),11*R*,20*S*-11,20,25-trihydroxy-3,4-*seco*-dammara-4(28),23-dien-3-oic acid methyl ester.

Qingqianliusu D (**4**), colorless amorphous powder with [α] 23 D = + 36.0 (*c* 0.25, MeOH). The HR-ESI-MS spectrum (**Fig. S33**) of **4** showed a quasi-molecular ion peak at *m/z* $[M + Na]^+$ at *m/z* 527.3719 (calcd. for $C_{31}H_{52}O_5Na$, 527.3712), which illustrated a molecular formula $C_{31}H_{52}O_5$. The ^1H and ^{13}C NMR data (Tables 1 and 2) of **4** were closely identical to **3** except for the side chain at C-17. A pair of terminal disubstitutd double bond carbon singlets at δ_C 148.8 (C-25) and δ_C 111.6 (C-26), one quaternary oxygen-bearing carbon at δ_C 75.6 (C-20), together with one oxygenated methine at δ_C 77.4 (C-24) suggested that compound **4** and **2** have the same side chain connected at C-17 (Table 2). Consequently, compound **4** was deduced as 11*R*,20*S*,24*S*-trihydroxy-3,4-*seco*-dammara-4(28),25-dien,3-oic acid methyl ester.

Qingqianliusu E (**5**) was isolated as a white amorphous powder with [α]23 D = + 39.4 (*c* 0.33, MeOH), which has the same molecular formula of $C_{31}H_{52}O_5$ as **4,** as evidenced by the ^{13}C spectrum (**Fig. S46**) and its sodium adduct molecular ion $[M + Na]^+$ at *m/z* 527.3717 (calcd. for $C_{31}H_{52}O_5Na$, 527.3712) in the HR-ESI-MS spectrum (**Fig. S42**). The ^1H and ^{13}C NMR (Tables 1 and 2) of **5** showed almost identical with **4** except for a slight difference in the chemical shifts [$\Delta\delta_C$ = δ_C (**5**) - δ_C (**4**)] at C-25 ($\Delta\delta_C$ + 0.35), C-26 ($\Delta\delta_C$ −0.30), and C-27 ($\Delta\delta_C$ + 0.31), which could be attributed to the difference configuration of the hydroxyl group (−OH) at C-24. Therefore, compound **5** was found to be epimer of **4** at C-24 according to spectroscopic data and characterized as 11*R*,20*S*,24*R*-trihydroxy-3,4-*seco*-dammara-4(28),25-dien,3-oic acid methyl ester.

Qingqianliusu F (**6**) was also obtained as white amorphous powder with [α]23 D = + 39.9 (*c* 0.28, MeOH). The molecular formula $C_{31}H_{52}O_4$ was confirmed by the HR-ESI-MS *m/z* 511.3764 $[M + Na]^+$ (calcd. for $C_{31}H_{52}O_4Na$, 511.3763) (**Fig. S51**) and ^{13}C NMR data (Table 2). Comprehensive analysis of the NMR data (Tables 1 and 2) of **5** and **6** revealed that compound **6** has one more methylene (δ_H 1.44/1.36, δ_C 23) while one less oxymethine (δ_H 3.91, δ_C 71.6). Moreover, the diagnostic ^1H–^1H COSY spectrum (**Fig. S56**) of δ_H 1.60 (m, H-9) and δ_H 1.44/1.36 (m, H_2-11) indicated that there was

no hydroxyl group substitutied at C-11. Therefore, the structure of **6** was determined as 20*S*,24*R*-dihydroxy-3,4-*seco*-dammara-4(28),25-dien,3-oic acid methyl ester.

Qingqianliusu G (**7**) was separated as white amorphous powder with [α]23 D = + 36.0 (*c* 0.22, MeOH), which had a molecular formula of $C_{30}H_{50}O_4$ determined by its quasi-molecular ion peak $[M + Na]^+$ at *m*/*z* 497.3589 (calcd. for $C_{30}H_{50}O_4Na$, 497.3607) in the HR-ESI-MS (**Fig. S60**), 14 mass units less than those of **6**. The ^1H and ^{13}C NMR spectral data (Tables 1 and 2) of **7** were also very similar to those of **6**, except for the disappearance of one methoxyl group. As a result, compound **7** was deduced as 20*S*,24*R*-dihydroxy-3,4-*seco*-dammara-4(28),25-dien,3-oic acid.

Qingqianliusu H (**8**), a white amorphous powder with [α]23 D = + 14.3 (*c* 0.21, MeOH), had the molecular formula $C_{30}H_{48}O_5$ by the ^{13}C NMR data (**Fig. S73**) and quasi-molecular ion peak $[M + Na]^+$ at *m*/*z* 511.3382 (calcd. for $C_{30}H_{48}O_5Na$, 511.3399) in the HR-ESI-MS (**Fig. S69**). The IR absorption (**Fig. S71**) at 3432, 2868, 1708 and 1692 cm^{-1} represented the presence of hydroxyl (—OH), aldehyde (—CHO) and carbonyl groups (—COOH), respectively. Analysis of the 1D and 2D NMR data (Tables 1 and 2) showed **8** was the high similarity with those of the know compound 20*S*,24*S*-dihydroxy-3,4-*seco*-dammara-4(28),25-dien, 3-oic acid **(15)**. The only slight difference in the group observed was the methyl group (—CH_3) in **15** replaced by the aldehyde group (—CHO) in **8** at C-4. The correlations from δ_H 6.42 (H-28a)/6.22 (H-28b) to δ_C 196.6 (C-29)/40.2 (C-5) in the HMBC spectrum (**Fig. S1** and **Fig. S76**) proved the linkage of aldehyde group located at C-4. These data generated the assignment of **8** as 20*S*,24*S*-dihydroxy-3,4-*seco*-dammara-4(28),25-dien,4-aldehyde group,3-oic acid.

Qingqianliusu I (**9**) was isolated as a colorless amorphous powder with [α]23 D = + 33.2 (*c* 0.21, MeOH). The molecular formula of **9** was determined to be $C_{32}H_{54}O_5$ by ^{13}C NMR spectrum (**Fig. S82**) and positive-ion peak $[M + Na]^+$ at *m*/*z* 541.3869 (calcd. for $C_{32}H_{54}O_5Na$, 541.3868) in the HR-ESI-MS (**Fig. S78**). The 1D and 2D NMR data (Tables 1 and 2) were nearly identical with cyclocariol E (**18**) (Chen et al., 2018), except for the replacement of the methoxy moiety (—OCH_3) by ethoxy unit (—OCH_2CH_3) at C-3 in **9**. Furthermore, the crucial ^1H–^1H COSY (**Fig. S83**) correlation of **9** illustrated the presence of ethyl fragment δ_C 4.11 (H-3-COO$\underline{CH_2}$$CH_3$) and 1.24 (H-3-$COOCH_2\underline{CH_3}$). In its key HMBC correlation (**Fig. S85**) from δ_H 4.11 (H-3-COO$\underline{CH_2}$$CH_3$) to δ_C 175.8 (C-3) suggested that ester ethyl unit (—OCH_2CH_3) at C-3. Therefore, the structure of **9** was determined as 23(*E*),12*R*,20*S*-11,20,25-trihydroxy-3,4-*seco*-dammara-4(28),23-dien-3-oic acid ethyl ester.

Qingqianliusu J (**10**), a white amorphous powder with [α]23 D = + 7.2 (*c* 0.29, MeOH), was assigned as molecular formula of $C_{39}H_{64}O_{10}$ determined on the basis of a positive-ion peak $[M + Na]^+$ *m*/*z* 715.4400 (calcd. for $C_{39}H_{64}O_{10}Na$, 715.4397) in the HR-ESI-MS (**Fig. S87**). A detailed analysis of 1D NMR data (Table 1 and Table 2), compound **10** were almost similar to **9** except for the additional glycosyl derivatives unit, which was proven by presence seven carbon singlets including one carbonyl signal at δ_H 172.6 (C-5′–O$\underline{CO}$$CH_3$); four oxygenated methines at δ_H 103.5 (C-1′), 83.7 (C-2′), 82.1 (C-4′), and 77.9 (C-3′); one oxygenated methylene at 65.2 (C-5′); and one methyl signal at δ_H 20.7 (C-5′–OCO$\underline{CH_3}$). The glycosyl unit can be identified as α-arabinose by comparing the ^{13}C NMR data with known compound cyclocarioside O (Liu et al., 2020). In addition, an acetoxy group (—$OCOCH_3$) attached to the C-5′ of α-arabinose based on the HMBC correlations (**Fig. S1** and **Fig. S94**) of δ_H 4.26 (H-5′a)/4.13 (H-5′b) with δ_C 172.6 (C-5′–O$\underline{CO}$$CH_3$). Then, the key HMBC correlations from anomeric hydrogen δ_H 5.27 (H-1′) with δ_C 83.8 (C-20) determined the position of glycosyl unit was located at C-20. Besides, the sugar was recognized with acid hydrolysis and HPLC analysis (**Fig. S5**) of L-arabinose standard. Therefore, the structure of **10** was deduced as 23(*E*),12*R*,20*S*-12,20,25-trihydroxy-3,4-*seco*-dammara-4(28),23-dien,3-oic acid ethyl ester-20-*O*-α-L-(5′-*O*-acetyl)-arabinofuranoside.

Qingqianliusu K (**11**) was deduced as a white amorphous powder with [α]23 D = + 12.0 (*c* 0.25, MeOH). The molecular formula of **11**, $C_{41}H_{68}O_{10}$, yielded a positive sodium ion HR-ESI-MS peak (**Fig. S96**) at *m*/*z* 743.4718 $[M + Na]^+$ (calcd. for $C_{41}H_{68}O_{10}Na$, 743.4710), which is 28 Da more than that of **10**. Detailed comparison of the ^1H and ^{13}C NMR data (Tables 1 and 2) showed that **11** was almost similar to **10,** except for the hydroxyl group (–OH) at C-25 was replaced by the ethoxy (–OCH_2CH_3), which was proven by the key HMBC correlations (**Fig. S103**) from δ_H 3.39 (H-25-O$\underline{CH_2}$$CH_3$) to δ_C 76.3 (C-25). In addition, the glycosyl unit was assigned as α-L-arabinofuranoside based on acid hydrolysis and HPLC analysis (**Fig. S5**). Therefore, compound **11** was a characteristic 3,4-*seco*-dammarane triterpenoid glycoside named as 23(*E*),12*R*,20*S*-12,20,25-trihydroxy-3,4-*seco*-dammara-4(28),23-dien,3-oic acid ethyl ester-25-*O*-ethyl,20-*O*-α-L-(5′-*O*-acetyl)-arabinofuranoside.

Qingqianliusu L (**12**) was obtained as a white amorphous powder and had a molecular formula of $C_{32}H_{54}O_5$, which

Table 3 Comparison of ^{13}C NMR spectroscopic of the isomers with **24*R*/24*S*** (CD_3OD, 150 MHz).

No.	Epimer (1)			Epimer (2)			Epimer (3)			Epimer (4)		
	17 (24*R*)	**16** (24*S*)	$\Delta\delta_C$ (24*R*-24*S*)	**13** (24*R*)	**12** (24*S*)	$\Delta\delta_C$ (24*R*-24*S*)	**7** (24*R*)	**15** (24*S*)	$\Delta\delta_C$ (24*R*-24*S*)	**5** (24*R*)	**4** (24*S*)	$\Delta\delta_C$ (24*R*-24*S*)
25	149.26	148.85	0.41	149.24	148.85	0.39	148.99	148.79	0.20	149.14	148.79	0.35
26	111.10	111.44	−0.34	111.10	111.44	−0.34	111.27	111.61	−0.34	111.30	111.60	−0.30
27	17.92	17.67	0.25	17.94	17.67	0.27	17.81	17.49	0.32	17.83	17.52	0.31

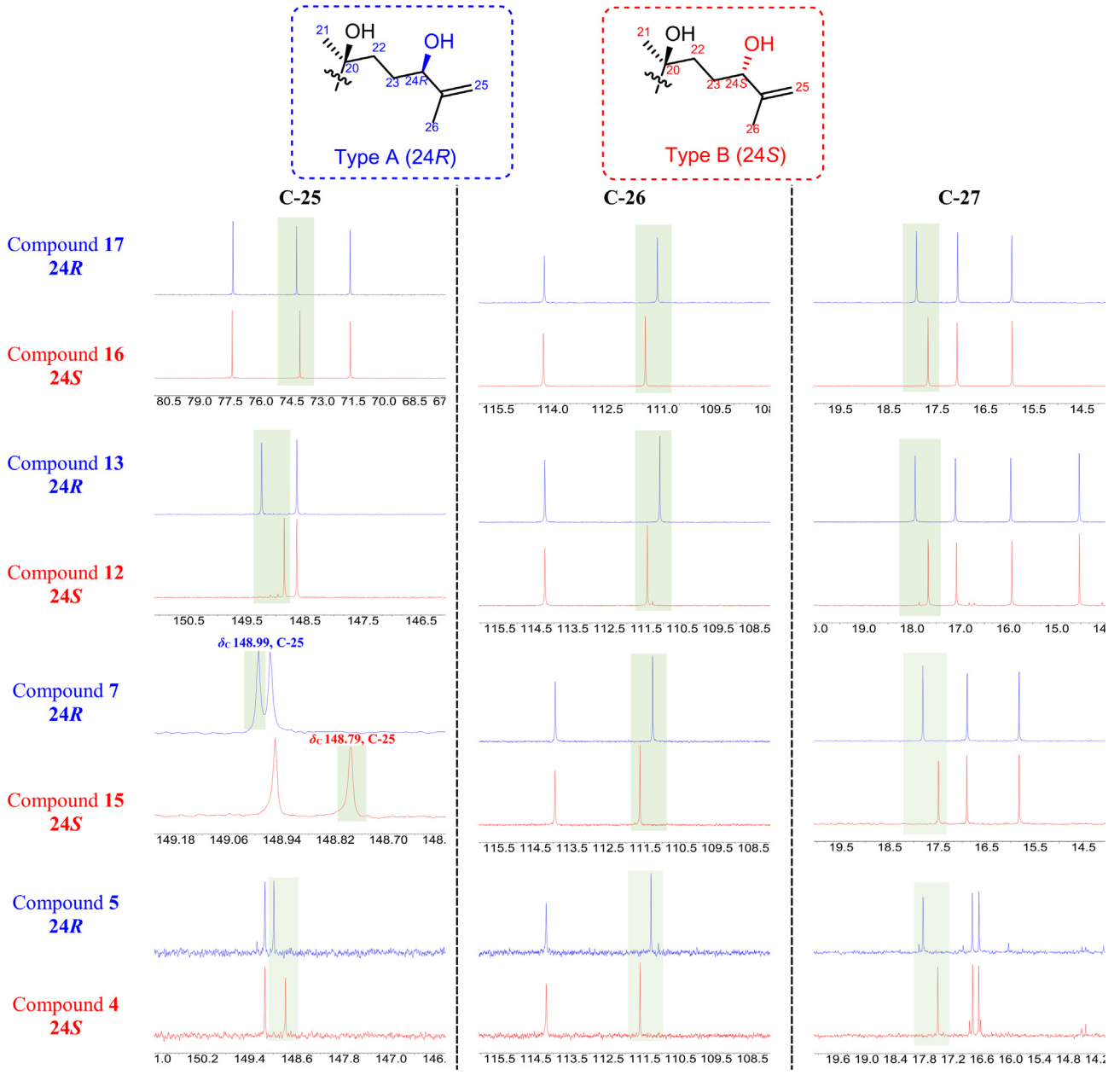

Fig. 4 Comparison of key ^{13}C NMR data differences for the isomers **24*R*** (represented in blue) and **24*S*** (represented in red) (CD_3OD, 150 MHz).

was established by HR-ESI-MS (Fig. S105) from a positive sodium ion at *m/z* 541.3863 $[M + Na]^+$ (calcd. for $C_{32}H_{54}O_5$-Na, 541.3869). Comparing the ^1H and ^{13}C NMR data (Tables 1 and 2) of **12** and cyclocariol B (**16**)(Chen et al., 2018), which demonstrated a considerable degree of similarity except for the replacement of the ester methoxy moiety (—OCH_3) by ethoxy unit (—OCH_2CH_3) at C-3 in **12**. Accordingly, the structure of **12** was deduced as 12*R*,20*S*,24*S*-trihydroxy-3,4-*seco*-dammara-4(28),25-dien,3-oic acid ethyl ester.

Qingqianliusu M (**13**), a white amorphous powder with [α] 23 D = + 40.8 (*c* 0.59, MeOH), had a molecular formula of $C_{32}H_{54}O_5$, the same as that **12**, as determined by the $[M + Na]^+$ ion peaks at *m/z* 517.3859 (calcd. for $C_{32}H_{54}O_5$-Na, 541.3869) in the HR-ESI-MS (Fig. S114). Detailed analysis of 1D NMR spectroscopic (Tables 1 and 2), compound **13** contained exactly a 3,4-*seco*-dammarane triterpenoids skeleton as **12**, except for a slight difference in the chemical shifts [$\Delta\delta_C = \delta_C$ (**13**) - δ_C (**12**)] at C-25 ($\Delta\delta_C$ + 0.39), C-26 ($\Delta\delta_C$ −0.34), and C-27 ($\Delta\delta_C$ + 0.27), which suggested that **13** was a epimer at C-24 of **12**. Therefore, compound **13** was elucidated as 12*R*,20*S*,24*R*-trihydroxy-3,4-*seco*-dammara-4(28),25-dien,3-oic acid ethyl ester.

Qingqianliusu N (**14**) was obtained as a white amorphous powder with [α]23 D = + 7.2 (*c* 0.28, MeOH). It provided the molecular formula $C_{39}H_{64}O_{10}$, which was determined by HRESI-MS ion $[M + Na]^+$ at *m/z* 715.4382 (calcd. for C_{39}-$H_{64}O_{10}Na$, 715.4397) (Fig. S123). The 1D NMR data (Tables 1 and 2) of **14** were highly analogous to those of **13** except for

Table 4 α-Glucosidase inhibition activities of compounds **1**–**14** *in vitro*.

compounds[a]	IC $_{50}$ (μM)[b]
8	4.97 ± 0.63
10	19.62 ± 0.70
11	7.08 ± 0.53
14	3.76 ± 0.77
Acarbose[c]	1.07 ± 0.31

[a] Compounds that are not shown in this table did not exhibit activity.
[b] Data expressed as means ±sD (n = 3).
[c] Acarbose was used as a positive control.

Table 5 COX-2 inhibitory rates of compounds **1**–**14** *in vitro*.

Compounds[a]	Sample concentration (μM)	Inhibition rate (%)
1	25	12.11
2	25	15.73
4	25	10.23
6	25	20.62
10	25	17.44
11	25	35.83
Celecoxib[b]	1	70.28

[a] Compounds that are not shown in this table did not exhibit activity.
[b] Celecoxib was used as a positive control.

the additional glycosyl derivatives unit, which indicated that **14** also possesses a 3,4-*seco*-dammarane triterpenoids skeleton. The glycosyl unit of **14** was identified as α-(5′-*O*-acetyl)-arabinofuranoside by comparing the ^{13}C data (Table 2) of compounds **10** and **11**. Moreover, the acid hydrolysis results were also in agreement with the presence of L-arabinofuranoside standard (**Fig. S5**). Thus, **14** was identified as 12*R*,20*S*,24*R*-trihydroxy-3,4-*seco*-dammara-4(28),25-dien,3-oic acid methyl ester-20-*O*-α-L-(5′-*O*-acetyl)-arabinofuranoside.

3.2. Determination of the absolute configurations of isomers

To further clarify the absolute configuration of the hydroxyl group (—OH) substituted at the C-24, according to the ^{13}C NMR date (Table 2) of C-25 to C-27 in the four pairs of epimers 24R/24S (**17**/**16**, **13**/**12**, **7**/**15**, and **5**/**4**) were compared and analyzed. One pair of known isomers cyclocariol B (**16**) and cyclocariol A (**17**) has been isolated by our group. The X-ray crystallographic analysis of **17** demonstrated that the absolute configuration at C-24 was *R*. As shown in Table 3 and Fig. 4, the rules demonstrated that the slight variations between the epimers were the chemical shifts (**24*R*-24*S***) at C-25 ($\Delta\delta_C$ + 0.20 to + 0.41), C-26 ($\Delta\delta_C$ −0.34 to −0.30), and C-27 ($\Delta\delta_C$ + 0.25 to + 0.32). Apparently, it could be basically inferred that compounds **5**, **7**, and **13** were found to be *R* configuration at C-24, while its corresponding epimers **4**, **15**, and **12** were in the *S* configuration.

3.3. α-Glucosidase inhibitory activity assay

Diabetes mellitus is a complex chronic metabolic disorder with an increasing prevalence every year (Xiao et al., 2017; Zhu et al., 2015). The inhibitors of α-glucosidase had become one of the clinically effective drugs for the prevention and treatment of diabetes (Chen et al., 2021; Li et al., 2012). On this basis, in order to further explore the potential hypoglycemic effect of the active components in Qingqianliu, α-glucosidase inhibitory activity was tested on fourteen 3,4-*seco*-dammarane triterpenoids (**1**–**14**). The results (Table 4) showed that only three compounds **8**, **11**, and **14** exhibited strong α-glucosidase inhibitory activities with the IC_{50} ranges from 3.76 ± 0.77 to 7.08 ± 0.53 μM, while compound **10** showed weak activity with IC_{50} value of 19.62 ± 0.70 μM, as compared with positive control acarbose (IC_{50} 1.07 ± 0.31 μM). The structure–activity relationship analysis indicated that the presences of the aldehyde group at C-4 and arabinose unit at C-20 could improve the α-glucosidase inhibitory activity.

3.4. Anti-inflammatory activity against COX-2

COX-2, known as Prostaglandin-endoperoxide synthase (PTGS), keeps closely related to the occurrence of inflammation and tumors (Jiang et al., 2022). The inhibitors of COX-2, which become a hot spot in drug research, could prevented inflammation and the formation of malignant tumors by blocking prostaglandin synthesis (Liu et al., 2020; Shataer et al., 2021). With celecoxib as positive control, the COX-2 inhibitory activity of compounds (**1**–**14**) were evaluated. The results were demonstrated in the Table 5. Only six compounds

Table 6 Cytotoxicities of compounds **1**–**14** against BGC-823, MCF-7, HCT-116 and Hepg-2 cell lines.

Compounds[b]	Cell lines (IC_{50} values, μM[a])			
	BGC-823	MCF-7	HCT-116	HepG-2
3	7.69 ± 0.21	>20	9.45 ± 0.93	>20
7	8.47 ± 0.41	>20	>20	>20
10	9.04 ± 0.61	>20	>20	>20
12	>20	>20	11.24 ± 0.22	>20
13	8.86 ± 0.38	9.19 ± 0.78	8.80 ± 0.36	13.41 ± 0.90
Paclitaxel[c] (nM)	8.93 ± 0.75	11.53 ± 0.26	14.71 ± 0.85	13.27 ± 1.18

[a] Compounds that are not shown in this table did not exhibit activity.
[b] Data expressed as means ± SD (n = 3).
[c] Taxol was used as a positive control.

1, **2**, **4**, **6**, **10**, and **11** showed COX-2 inhibitory activity with inhibition rates from 10.23 % to 35.83 % at the concentration of 25 μM. Among them, compound **11** had the highest inhibition rate and reached half of the inhibition rate of celecoxib. The results indicated that an additional sugar moiety at C-20 plays an important role in COX-2 inhibitory activity.

3.5. Cytotoxic bioassays

All unreported 3,4-*seco*-dammarane triterpenoids (**1**–**14**) were evaluated for their cytotoxicities against for human cancer cell lines (BGC-823, MCF-7, HCT-116, and HepG-2). As shown in Table 6, compounds **3**, **7**, **10**, and **13** displayed moderate activities against BGC-823 with IC_{50} values from 7.69 ± 0.21 to 9.04 ± 0.61. Moreover, compound **13** showed modest activity against MCF-7 and HCT-116 with IC_{50} values of 9.19 ± 0.78 and 8.80 ± 0.36. respectively. Structurally, compounds **13** and **12** as a pair of isomers, which **13** exhibited stronger activities than **12**. It can be inferred that the hydroxyl group at the C-24 was *R* configuration in the same type of 3,4-*seco*-dammarane triterpenoids skeleton possess potential cytotoxicity effect.

4. Conclusion

In conclusion, as a new raw food material with the edible and medicinal values, the investigations of chemical constituents with bioactive effects in Qingqianliu keeps urgently needed. In this study, fourteen new 3,4-*seco*-dammarane triterpenoids (**1**–**14**) and four known 3,4-*seco*-dammarane triterpenoids (**15**–**18**) were isolated and identified. Notably, two 3,4-*seco*-dammarane triterpenoids (**1** and **2**) with the rare structural features of heptacyclic lactone linked by oxygen between C-3 and C-11 in parent were obtained. Furthermore, three compounds (**10**, **11,** and **14**) with their sugar units were attached to the C-20 while most at C-11 and C-12 were also found. Four compounds (**6**–**8** and **15**) were rare 3,4-*seco*-dammarane triterpenoids without hydroxyl at position C-11 and C-12. In addition, the NMR data rules of determining the absolute configuration of four pairs of epimers at C-24 were discovered and summarized for the first time.

All undescribed compounds were calculated for anti-hypoglycemic, anti-inflammatory, and cytotoxic activities *in vitro*. Compounds **8**, **11**, and **14** exhibited good α-glucosidase inhibitory activity compared with the positive control acarbose. Compound **10** showed a weak inhibitory effect on α-glucosidase and COX-2, together with strong inhibitory activity on BGC-823, respectively. These studies provided a preliminary biological activity basis for the anti-hyperglycemia, anti-inflammatory, and cytoxicity latent impacts of Qingqianliu, and furnished references for its development and utilization as functional foods or medicines.

Declaration of Competing Interest

The authors declare that they have no known competing financial interests or personal relationships that could have appeared to influence the work reported in this paper.

Acknowledgements

This work was financially supported by the National Natural Science Foundation of China (No. 82174078, 81803708, 81874369, and 82074122); Changjiang Scholars Program in Ministry Education, People's Republic of China (T2019133); and Hunan Administration of Tradition Chinese Medicine (Xiangcai2021-105).

Appendix A. Supplementary material

Supplementary data to this article can be found online at https://doi.org/10.1016/j.arabjc.2022.104441.

References

Aoki, T., Ohta, S., Suga, T., 1988. Six novel secodammarane-type triterpenes from male Flowers of *Alnus japonica*. Phytochemistry 27 (9), 2915–2920.

Aoki, T., Ohta, S., Suga, T., 1990. Triterpenoids, diarylheptanoids and their glycosides in the flowers of *Alnus species*. Phytochemistry 29 (11), 3611–3614.

Chai, X.Y., Song, Y.L., Xu, Z.R., Shi, H.M., Bai, C.C., Bi, D., Wen, J., Li, F.F., Tu, P.F., 2008. Itosides J-N from Itoa orientalis and structure - anti-COX-2 activity relationship of phenolic glycosides. J. Nat. Prod. 71 (5), 814–819.

Chen, S.H., Li, Z., Li, W.J., Huang, Z.Z., Jia, Q., 2021. Confining copper nanoclusters on exfoliation-free 2D boehmite nanosheets: fabrication of ultra-sensitive sensing platform for α-glucosidase activity monitoring and natural anti-diabetes drug screening. Biosens. Bioelectron. 182, 113198. https://doi.org/10.111016/j.bios.112021.113198.

Chen, Z.L., Jian, Y.Q., Wu, Q., Wu, J., Sheng, W.B., Jiang, S., Shehla, N., Aman, S., Wang, W., 2022. *Cyclocarya paliurus* (Batalin) Iljinskaja: Botany, Ethnopharmacology, phytochemistry and pharmacology. J. Ethnopharmacol. 285, 114912.

Chen, Y.J., Na, L., Fan, J., Zhao, J., Hussain, N., Jian, Y.Q., Yuan, H., Li, B., Liu, B., Choudhary, M.I., Khan, I., Wang, W., 2018. *Seco*-dammarane triterpenoids from the leaves of *Cyclocarya paliurus*. Phytochemistry 145, 85–92.

Cui, B.S., Li, S., 2012. Chemical constituents from leaves of *Cyclocarya paliurus*. Chin. Tradit. Herb. Drug 43 (11), 2132–2136.

Gao, Y., He, C.N., Bi, W., Wu, G.F., Altman, E., 2016. Bioassay Guided Fractionation Identified Hederagenin as a Major Cytotoxic Agent from *Cyclocarya paliurus* Leaves. Planta Med. 82 (1–2), 171–179.

Jiang, W.H., Jin, Y.Y., Zhang, S.W., Ding, Y., Huo, K.L., Yang, J.J., Zhao, L., Nian, B.N., Zhong, T.P., Lu, W.Q., Zhang, H.K., Cao, X., Shah, K.M., Wang, N., Liu, M.Y., Luo, J., 2022. PGE_2 activates EP_4 in subchondral bone osteoclasts to regulate osteoarthritis. Bone Res. 10 (1), 27.

Kennelly, E.J., Cai, L., Long, L., Shamon, L., Zaw, K., Zhou, B.N., Pezzuto, J.M., Kinghorn, A.D., 1995. Novel Highly Sweet Secodammarane Glycosides from *Pterocarya paliurus*. J. Agric. Food Chem. 43 (10), 2602–2607.

Li, S., Cui, B.S., Liu, Q., Tang, L., Yang, Y.C., Jin, X.J., Shen, Z.F., 2012. New Triterpenoids from the Leaves of *Cyclocarya paliurus*. Planta Med. 78 (03), 290–296.

Li, C.G., Deng, S.P., Liu, W., Zhou, D.X., Huang, Y., Liang, C.Q., Hao, L.L., Zhang, G.R., Su, S.S., Xu, X., Yang, R.Y., Li, J., Huang, X.S., 2021. α-Glucosidase inhibitory and anti-inflammatory activities of dammarane triterpenoids from the leaves of *Cyclocarya paliurus*. Bioorg. Chem. 111, 104847.

Liu, W., Deng, S.P., Zhou, D.X., Huang, Y., Li, C.G., Hao, L.L., Zhang, G.R., Su, S.S., Xu, X., Yang, R.Y., Li, J., Huang, X.S., 2020. 3,4-*seco*-Dammarane Triterpenoid Saponins with Anti-Inflammatory Activity Isolated from the Leaves of *Cyclocarya paliurus*. J. Agric. Food Chem. 68 (7), 2041–2053.

Ning, Z.W., Zhai, L.X., Huang, T., Peng, J., Hu, D., Xiao, H.T., Wen, B., Lin, C.Y., Zhao, L., Bian, Z.X., 2019. Identification of alpha-glucosidase inhibitors from *cyclocarya paliurus* tea leaves using UF-

UPLC-Q/TOF-MS/MS and molecular docking. Food Funct. 10 (4), 1893–1902.

Peng, W.W., Zhao, S.M., Ji, C.J., Huo, G.H., Wan, C.P., Li, Y.Y., Zhang, Y.L., 2019. Cyclopalitins A and B, nortriterpenoids from aerial parts of *Cyclocarya paliurus*. Phytochem. Lett. 31, 114–117.

Perez, J.L., Jayaprakasha, G.K., Patil, B.S., 2019. Metabolite profiling and in vitro biological activities of two commercial bitter melon (*Momordica charantia* Linn.) cultivars. Food Chem. 288, 178–186. https://doi.org/10.1016/j.foodchem.2019.1002.1120.

Phan, M.G., Truong, T.T.C., Phan, T.S., Matsunami, K., Otsuka, H., 2011. Three new dammarane glycosides from *Betula alnoides*. Phytochem. Lett. 4 (2), 179–182.

Shataer, D., Li, J., Duan, X.M., Liu, L., Xin, X.L., Aisa, H.A., 2021. Chemical Composition of the Hazelnut Kernel (*Corylus avellana L.*) and Its Anti-inflammatory, Antimicrobial, and Antioxidant Activities. J. Agric. Food Chem. 69 (14), 4111–4119.

Shen, B.B., Chen, S.H., Zhou, Q., Jian, Y.Q., Daniyal, M., Sheng, W. B., Gong, L.M., Luo, D.X., Liu, B., Xu, G.M., Wang, W., 2020. Flavonoid glycosides from the rhizomes of *Pronephrium penangianum*. Phytochemistry 179, 112500. https://doi.org/10.111016/j.phytochem.112020.112500.

Smirnova, I.E., Petrova, A.V., Kazakova, O.B., Minnibaeva, E.M., Fedorova, A.A., Van, L.E., Van, C.T., Thi, N.P., Phuong, T.T.T., Thi, D.N., 2020. Synthesis of dammarenolic acid derivatives with a potent α-glucosidase inhibitory activity. Med. Chem. Res. 29 (4), 1–9.

Sun, H.H., Tan, J., Lv, W.Y., Li, J., Wu, J.P., Xu, J.L., Zhu, H., Yang, Z., Wang, W., Ye, Z., Xuan, T., Zou, Z., Chen, Z., Xu, K., 2020b. Hypoglycemic triterpenoid glycosides from *Cyclocarya paliurus* (Sweet Tea Tree). Bioorg. Chem. 95, 103493. https://doi.org/10.101016/j.bioorg.102019.103493.

Sun, H.H., Lv, W.Y., Tan, J., Tang, Y.C., Zhu, H., Qu, J.B., Li, J., Wu, J.P., Chang, X.W., Yang, Z.C., Wang, W.X., Chen, Z.H., Xu, K.P., 2020a. Cytotoxic triterpenoid glycosides from leaves of *Cyclocarya paliurus*. Nat. Prod. Res. 35 (21), 4018–4024.

Sun, H.H., Zhu, H., Wu, J.P., Wang, Y.Y., Li, G.H., Liu, Y.Q., Chang, X.W., Ou, S.Y., Zha, W.W., Chen, H.Y., Gui, R., He, X. A., Lu, S.J., Shangguan, D.G., Xu, K.P., 2021. Two new triterpenoid glycosides from leaves of *Cyclocarya paliurus*. Nat. Prod. Res., 1–6

Takayuki, S., Toshifumi, H., 1979. New C_{31} Secodammarane-type Triterpenoids, Alnuseric Acid and Alniselide, in the Male Flowers of *Alnus serrulatoides*. Bull. Chem. Soc. Jpn. 52 (4), 1153–1155.

Wu, Z.F., Gao, T.H., Zhong, R.L., Lin, Z., Jiang, C.H., Ouyang, S., Zhao, M., Che, C.T., Zhang, J., Yin, Z.Q., 2017. Antihyperlipidaemic effect of triterpenic acid-enriched fraction from *Cyclocarya paliurus* leaves in hyperlipidaemic rats. Pharm. Biol. 55 (1), 712–721.

Xiao, H.T., Wen, B., Ning, Z.W., Zhai, L.X., Liao, C.H., Lin, C.Y., Mu, H.X., Bian, Z.X., 2017. *Cyclocarya paliurus* tea leaves enhances pancreatic beta cell preservation through inhibition of apoptosis. Sci. Rep. 7 (1), 9155.

Xie, J.H., Xie, M.Y., Nie, S.P., Shen, M.Y., Wang, Y.X., Li, C., 2010. Isolation, chemical composition and antioxidant activities of a water-soluble polysaccharide from *Cyclocarya paliurus* (Batal.) Iljinskaja. Food Chem. 119 (4), 1626–1632.

Xie, J.H., Dong, C.J., Nie, S.P., Li, F., Wang, Z.J., Shen, M.Y., Xie, M.Y., 2015. Extraction, chemical composition and antioxidant activity of flavonoids from *Cyclocarya paliurus* (Batal.) Iljinskaja leaves. Food Chem. 186, 97–105.

Xie, J.H., Wang, W.J., Dong, C.J., Huang, L.X., Wang, H., Li, C., Nie, S.P., Xie, M.Y., 2018. Protective effect of flavonoids from *Cyclocarya paliurus* leaves against carbon tetrachloride-induced acute liver injury in mice. Food Chem. Toxicol. 119, 392–399.

Yan, H.J., Wang, J.S., Kong, L.Y., 2014. Cytotoxic dammarane-type triterpenoids from the stem bark of *Dysoxylum binecteriferum*. J. Nat. Prod. 77 (2), 234–242.

Yang, Z.W., Wang, J., Li, J.G., Xiong, L., Chen, H., Liu, X., Wang, N., Ouyang, K.H., Wang, W.J., 2018. Antihyperlipidemic and hepatoprotective activities of polysaccharide fraction from *Cyclocarya paliurus* in high-fat emulsion-induced hyperlipidaemic mice. Carbohyd. Polym. 183, 11–20.

Yang, D.J., Zhong, Z.C., Xie, Z.M., 1992. Studies on the sweet principles from the leaves of *Cyclocarya paliurus*(Batal.) Iljinsk. Acta Pharm. Sin. 27 (11), 841–844.

Zhou, X.L., Li, S.B., Yan, M.Q., Luo, Q., Wang, L.S., Shen, L.L., Liao, M.L., Lu, C.H., Liu, X.Y., Liang, C.Q., 2021. Bioactive dammarane triterpenoid saponins from the leaves of *Cyclocarya paliurus*. Phytochemistry 183, 112618.

Zhu, K.N., Jiang, C.H., Tian, Y.S., Xiao, N., Wu, Z.F., Ma, Y.L., Lin, Z., Fang, S.Z., Shang, X.L., Liu, K., Zhang, J., Liu, B.L., Yin, Z. Q., 2015. Two triterpeniods from *Cyclocarya paliurus* (Batal) Iljinsk (Juglandaceae) promote glucose uptake in 3T3-L1 adipocytes: The relationship to AMPK activation. Phytomedicine 22 (9), 837–846.